BETATRON X-RAYS FROM A LASER WAKEFIELD ACCELERATOR IN THE IONIZATION INDUCED TRAPPING REGIME *

F. Albert, B.B. Pollock, Y.-H. Chen, D. Alessi, J.E. Ralph, P.A. Michel, A. Pak,
LLNL, Livermore, CA 94550, USA
J. Shaw, K.A. Marsh, C.E. Clayton, C. Joshi, UCLA, CA 90095, USA
S.H. Glenzer, SLAC, Stanford, CA 94309, USA

Abstract

Betatron x-rays with multi-keV photon energies have been observed from a GeV-class laser-plasma accelerator. The experiment was performed using the 200 TW Callisto laser system at LLNL to produce and simultaneously observe GeV-class electron beams and keV Betatron x-rays. The laser was focused into various gas cells with sizes ranging from 3 to 10 mm, and containing mixed gases (He, N, CO_2, Ar, Ne) to accelerate large amounts of charge in the ionization induced trapping regime. KeV betatron x-rays were observed for various concentrations of gases. Electron spectra were measured on large image plates with the two-screen method after being deflected by a large 0.42 Tesla magnet spectrometer.

INTRODUCTION

Laser Wakefield Acceleration (LWFA)[1] is one of the most notable applications of petawatt-class laser systems. Since the discovery that this mechanism can accelerate monoenergetic electron beams up to energies comparable to those obtained with conventional rf accelerators[2, 3, 4] but in a table-top setup, novel applications of these electron beams have been constantly increasing. Concurrently, x-ray sources such as synchrotrons, or more recently free-electrons lasers such as the Linac Coherent Light Source (LCLS)[5] continue to explore new properties of atoms, molecules, condensed matter, warm dense matter or plasmas. In this context, LWFA beams are very attractive to seed the next generation of light sources. Such beams can either be wiggled by an external periodic magnetic structure[6] or directly by the plasma in the wake of the laser pulse[7, 8] to produce keV x-rays. The latter example, the betatron x-ray source, first observed in a beam-driven plasma channel[9] is the subject of this work, and its mechanism can be described as follows: an ultrashort (femtosecond), ultraintense ($I > 10^{18}$ W/cm^2) laser pulse is focused under vacuum on the edge of a gas target. The gas is fully ionized to form a plasma. The laser ponderomotive force (proportional to the gradient of light intensity) plows the electrons of the plasma away from the strong light intensity regions. Because of the very short duration of the laser pulse, the heavier ions stay immobile and a bubble free of electrons is formed in the wake of the pulse. At the back of this bubble, some electrons are trapped, accelerated and wiggled by the electrical fields present in the plasma: these electrons emit the betatron x-rays. This source produces broadband, synchrotron-like radiation in the keV energy range[10, 11], within a source size of a few microns[12, 13], a divergence of less than 100 mrad[14], and a pulse duration of less than 100 fs[15]. Since betatron x-rays are directly related to the electrons emitting them, the source is also widely used as an electron beam diagnostic. The electron beam emittance and size can be deduced from the x-ray beam profile[14], spectrum[16] or source size[17], using various x-ray spectroscopy and imaging techniques. Traditionally, betatron x-rays are produced in the blowout regime of laser wakefield acceleration[18] using pure helium gas, where electrons are self-injected into the wake. This paper investigates the properties of betatron x-ray radiation produced in mixed gases.

BETATRON RADIATION MODELING

The motion of an electron accelerated along $\vec{u_z}$ with momentum $\vec{p}$ and position $\vec{r}$ in the wake of a laser pulse can be described by the Lorentz equation of motion:

$$\frac{d\vec{p}}{dt} = -m\omega_p^2 \frac{\vec{r}}{2} + \alpha \frac{mc\omega_p}{e}\vec{u_z}, \qquad (1)$$

where m is the electron rest mass, e the elementary charge, and $\omega_p = \sqrt{n_e e^2/m\epsilon_0}$ is the plasma frequency. Here, n_e is the electron density, and ϵ_0 the vacuum permittivity. In the blowout 3D nonlinear regime of laser wakefield acceleration [18], $\alpha = \frac{1}{2}\sqrt{a_0}$ is the normalized accelerating field, where a_0 is the laser normalized vector potential, typically around 2 for our experiments. Equation 1 can be solved by using a 4th order Runge-Kutta algorithm to obtain the single electron trajectories for given initial conditions and fields. The electron trajectory is used to calculate the intensity radiated by the particle per unit frequency ω and solid angle Ω [19]:

$$\frac{d^2 I}{d\Omega d\omega} = \frac{e^2\omega^2}{4\pi c}\left|\int_{-\infty}^{\infty} \vec{n} \times (\vec{n} \times \beta)\, e^{i\omega(t - \frac{\vec{n}.\vec{r}}{c})}dt\right|^2, \quad (2)$$

where $\vec{n}$ is the vector corresponding to the direction of observation, and $\beta = v/c$ the normalized electron velocity. The betatron x-ray beam profile is calculated by integrating Equation 2 over frequencies. Figure 1 shows an example of electron trajectory, with its corresponding betatron x-ray spectrum and beam profile. For this particular case, the parameters are $n_e = 10^{19}$ cm^{-3}, $\gamma = 200$, $x_0 = 1$ μm, $y_0 = 0$,
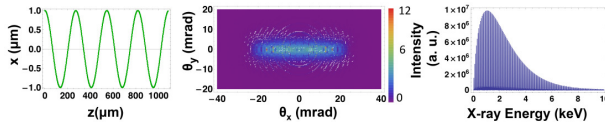
Figure 1: From left to right: example of an electron trajectory in the plasma, with the corresponding betatron spectrum observed on-axis and the x-ray beam profile.
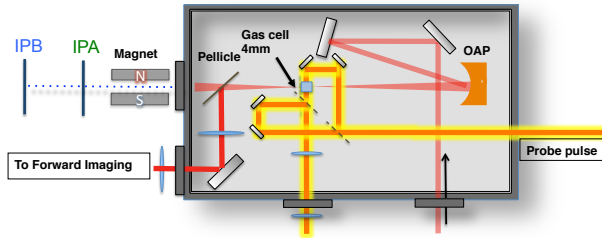

Figure 2: Experimental setup for betatron x-rays production and detection (see text for details).
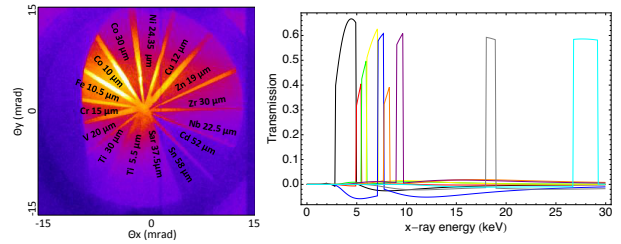

Figure 3: Betatron x-ray beam observed on IP_a through the pie-shaped set of filters (left) and corresponding Ross filter pairs used to measure the spectrum (right). Each pair corresponds to the difference of signal observed through two specific filters. The nine pairs (and their respective mean energy E_n and bandwidth ΔE_n) are, from low to high x-ray energy: 5.5 μm Ti and 37.5 μm Saran (3.9 keV, 2 keV), 20 μm V and 30 μm Ti (5.2 keV, 0.45 keV), 15 μm Cr and 20 μm V (5.7 keV, 0.45 keV), 10.5 μm Fe and 15 μm Cr (6.5 keV, 1.05 keV), 10 μm Co and 15 μm Fe (7.4 keV, 0.53 keV), 24.35 μm Ni and 30 μm Co (8.3 keV, 0.52 keV), 19 μm Zn and 17.5 μm Cu (9.3 keV, 0.6 keV), 22.5 μm Nb and 30 μm Zn (18.5 keV, 0.9 keV), 58 μm Sn and 52 μm Cd (28 keV, 2.3 keV).

and $\alpha = 0$. The trajectory was calculated using 3000 time steps (with each unit step $dt = 0.2c/\omega_p$). At each point of calculation of the trajectory, the spectrum and beam profile were calculated using frequency steps of 100 eV. For the chosen parameters, $\omega_c = 4.2$ keV and $K \simeq 6$. The beam has a divergence of $1/\gamma$ and K/γ along the direction parallel and perpendicular to the plane of the oscillations, and the on-axis spectrum peaks at ~ 2 keV. Although more computationally intensive, electrons trajectories obtained from PIC simulations can be post-processed using Equation 2 to calculate the spectrum and profile with a much better resolution[20].

EXPERIMENTAL SETUP

The experiments were conducted at the Jupiter Laser Facility (JLF) using the 200 TW Callisto laser system. Callisto can deliver up to 12 J in a 60 fs pulse (full width at half maximum, fwhm). The 13 cm diameter beam was focused by an off-axis parabola (f/8) onto the 500 μm entrance pinhole of a gas cell. The experimental setup is shown on Figure 2. The laser focal spot size w_0 was measured under vacuum at low power to be 12 μm. The back pinhole is 1 mm wide, and we have used different gas cell lengths (from 3 mm to 10 mm) as well as two-stage designs [21]. The cell was typically filled with He gas, but also with N, CO2, Ar and Ne. Electron densities ranging from 2×10^{18} cm^{-3} to 1.5×10^{19} cm^{-3} were measured for each shot with a 100 fs probe using interferometry in combination with an Abel-inversion code. The laser spot at the exit of the gas cell was imaged using a forward diagnostic, and spectrally resolved using grating and prism-based spectrometers. The electron beams were characterized using a two-screen spectrometer [22, 23]. This system provides an accurate measurement

of the energy of the electrons, the vertical and horizontal angle that the electrons exit the plasma relative to the original laser axis, the divergence, and the electron charge. The electrons exiting the plasma are deflected in the vertical direction by a 21-cm-long, 0.42 Tesla dipole magnet. The electrons are detected by two successive image plates (IP_a and IP_b) allowing for a unique solution to their energy and deflection, provided common spatial features can be identified on both image plates. Both the betatron x-ray beam profile and the x-ray spectrum were measured on the first image plate IP_a. At the vacuum/air interface, we used a 12 μm thick Al foil to block the 800 nm light from the laser as well as a 60 μm mylar window to hold vacuum. X-rays (profile or spectrum) are then measured on the image plate. To measure the x-ray spectrum from 1 keV to 30 keV, we used a set of Ross filter pairs, with transmission functions that provide narrow energy bands. The number of x-ray photons per unit energy is given by $N_{ph} = S_n/(T_n \Delta E_n)$, where S_n, T_n and ΔE_n are respectively the signal, transmission and bandwidth of a given energy band. Shown on Figure 3 is a typical x-ray beam observed on IP_a through the pie-shaped sets of filters, as well as the energy bands used in the experiment.

RESULTS AND DISCUSSION

Betatron x-rays where observed in different gases. For the different profiles shown in Figure 4, observed on IP_a through the filters, the x-rays where produced in a 4 mm gas cell containing mixed gases. Although these x-rays where produced in different gases, in order to make quantitative arguments it is important to note that they corre-

03 Alternative Acceleration Schemes

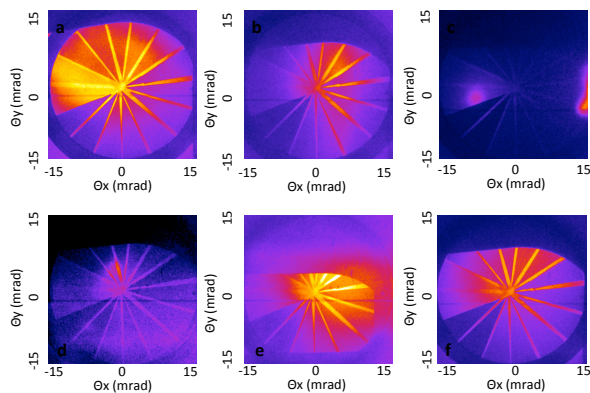A23 - Laser-driven Plasma Acceleration

Figure 4: Betatron x-ray beam beam profiles observed on IP_a through the pie-shaped set of filters (see text for details). The gas composition for each shot was (from top left, clockwise): 100% He, 95% He and 5% Ar, 80% He and 20 % N2, 80% He and 20 % N2, 98% He and 2% Ar, 95% Ar and 5% He.

spond to different electron beam energies. The electron beam maximum energy (the largest contribution to the x-rays) is, for each of these shots: 234 MeV, 300 MeV, 385 MeV, 186 MeV, 280 MeV, 125 MeV (from top left, clockwise). Electron densities were in the 5×10^{18}- 1×10^{19} cm^{-3} range for each of these shots and $2 < a_0 < 2.5$. In some cases (Figure 4) the beam profile could be very well observed on both IP_a and IP_b with a 25% transmission from IP_a to IP_b. According to the theoretical and experimental response function and transmission curve of the image plates[24], it means that the beam contains a large amount of x-rays with energies above 20 keV. For this particular case, the electron beam peaked at ~ 385 MeV, where most of the charge was located. Since the critical frequency scales with γ^2 and that in practical units, $\hbar\omega_c[\text{keV}]=5 \times 10^{-24} \times \gamma^2 n_e[\text{cm}^{-3}]r[\mu m]$, it means that for $n_e = 10^{19}$ cm^{-3} and $\gamma = 750$, $r \simeq 0.7$ μm when the electrons reach their end energy. The drawback of using filter wedges in our experiments was the beam pointing jitter. As observed on Figure 4, the beam center location varies up to a few milliradians around the filter tips. Since the x-ray intensity and energy strongly depend on the angle of observation (Equation 2), making quantitative statements about the x-ray spectrum requires x-ray measurements be made at the same angular position with respect to the beam center.

CONCLUSION AND PERSPECTIVES

In conclusion we have observed betatron x-rays at energies beyond 20 keV in a collimated beam with <30 mrad divergence. X-rays have been observed in pure He, but also in He/N and He/Ar mixes, which opens several possibilities to improve and control the x-ray flux and spectrum of the source. By taking advantage of electron acceleration in the ionization-induced trapping regime, large amounts of charge can be trapped and produce bright betatron x-rays. Our preliminary measurements support betatron oscillations of ~ 1 μm in the plasma, but also show that a simultaneous measurement of the x-ray beam profile and spectrum at a particular angle is necessary in order to make quantitative arguments about betatron x-rays production in this regime.

REFERENCES

[1] T.Tajima and J.M. Dawson *Phys. Rev. Lett.* **43**, 267–270 (1979).

[2] S. P. D. Mangles et al. *Nature* **431**, 535–538 (2004).

[3] C. G. R. Geddes et al. *Nature* **431**, 538–541 (2004).

[4] J. Faure et al. *Nature* **431**, 541–544 (2004).

[5] P. Emma et al. *Nat. Photon.* **4**, 641–647 (2010).

[6] M. Fuchs et al. *Nat. Phys.* **5**, 826–829 (2009).

[7] A. Rousse et al. *Phys. Rev. Lett.* **93**, 135005 (2004).

[8] S. Corde et al. *Rev. Mod. Phys.* **85**, 1–47 (2013).

[9] S. Wang et al. *Phys. Rev. Lett.* **88**, 135004 (2002).

[10] F. Albert et al. *Phys. Rev. E* **77**, 056402 (2008).

[11] S. Fourmaux et al. *New J. Phys.* **13**, 033017 (2011).

[12] R. C. Shah et al. *Phys. Rev. E* **74**, 045401(R) (2006).

[13] S. Kneip et al. *Nat. Phys.* **6**, 980–983 (2010).

[14] K. Ta Phuoc et al. *Phys. Rev, Lett* **97**, 225002 (2006).

[15] K. Ta Phuoc et al. *Phys. Plasmas* **14**, 080701 (2007).

[16] G. R. Plateau et al. *Phys. Rev. Lett.* **109**, 064802 (2012).

[17] S. Kneip et al. *Phys. Rev. ST Accel. Beams* **15**, 021302 (2012).

[18] W. Lu et al. *Phys. Rev. ST Acc. Beams* **10**, 061301 (2007).

[19] J.D. Jackson, [*Classical Electrodynamics*] (1998).

[20] J.L. Martins et al. *Proc. SPIE* **7359**, 73590V–1–73590V–8 (2009).

[21] B. B. Pollock et al. *Phys. Rev. Lett* **107**, 045001 (2011).

[22] B. B. Pollock et al. *Proceedings of PAC09, Vancouver, BC Canada*, 3035–3037 (2009).

[23] C. E. Clayton et al. *Phys. Rev. Lett* **105**, 105003 (2010).

[24] B. R. Maddox et al. *Rev. Sc. Instr.* **82**, 023111 (2011).